


## Article

# Metabolites with Anti-Inflammatory Activity from the Mangrove Endophytic Fungus *Diaporthe* sp. QYM12

Yan Chen <sup>1,2</sup>, Ge Zou <sup>2</sup>, Wencong Yang <sup>2</sup>, Yingying Zhao <sup>1</sup>, Qi Tan <sup>2</sup>, Lin Chen <sup>3</sup>, Jinmei Wang <sup>1</sup>, Changyang Ma <sup>1</sup>, Wenyi Kang <sup>1,\*</sup> and Zhigang She <sup>2,\*</sup> 

<sup>1</sup> National R & D Center for Edible Fungus Processing Technology, Henan University, Kaifeng 475004, China; chenyan27@mail2.sysu.edu.cn (Y.C.); zhaoyingying@vip.henu.edu.cn (Y.Z.); wangjinmei@henu.edu.cn (J.W.); macaya1024@vip.henu.edu.cn (C.M.)

<sup>2</sup> School of Chemistry, Sun Yat-Sen University, Guangzhou 510275, China; zoug5@mail2.sysu.edu.cn (G.Z.); yangwc6@mail2.sysu.edu.cn (W.Y.); tanq27@mail2.sysu.edu.cn (Q.T.)

<sup>3</sup> Henan Joint International Research Laboratory of Drug Discovery of Small Molecules, Zhengzhou Key Laboratory of Synthetic Biology of Natural Products, Huanghe Science and Technology College, Zhengzhou 450063, China; lchenchina@hsttu.edu.cn

\* Correspondence: kangwenyi@henu.edu.cn (W.K.); cesszhg@mail.sysu.edu.cn (Z.S.)

**Abstract:** One new diterpenoid, diaporpenoid A (**1**), two new sesquiterpenoids, diaporpenoids B–C (**2,3**) and three new  $\alpha$ -pyrone derivatives, diaporpyrones A–C (**4–6**) were isolated from an MeOH extract obtained from cultures of the mangrove endophytic fungus *Diaporthe* sp. QYM12. Their structures were elucidated by extensive analysis of spectroscopic data. The absolute configurations were determined by electronic circular dichroism (ECD) calculations and a comparison of the specific rotation. Compound **1** had an unusual 5/10/5-fused tricyclic ring system. Compounds **1** and **4** showed potent anti-inflammatory activities by inhibiting the production of nitric oxide (NO) in lipopolysaccharide (LPS)-induced RAW264.7 cells with IC<sub>50</sub> values of 21.5 and 12.5  $\mu$ M, respectively.

**Keywords:** mangrove endophytic fungus; *Diaporthe* sp.; anti-inflammatory activity



**Citation:** Chen, Y.; Zou, G.; Yang, W.; Zhao, Y.; Tan, Q.; Chen, L.; Wang, J.; Ma, C.; Kang, W.; She, Z. Metabolites with Anti-Inflammatory Activity from the Mangrove Endophytic Fungus *Diaporthe* sp. QYM12. *Mar. Drugs* **2021**, *19*, 56. <https://doi.org/10.3390/md19020056>

Academic Editor:

RuAngelie Edrada-Ebel

Received: 5 January 2021

Accepted: 21 January 2021

Published: 24 January 2021

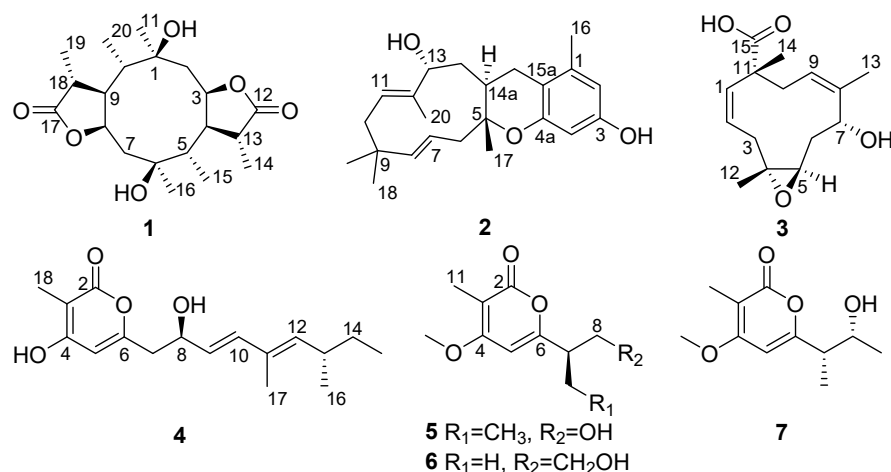
**Publisher's Note:** MDPI stays neutral with regard to jurisdictional claims in published maps and institutional affiliations.



**Copyright:** © 2021 by the authors. Licensee MDPI, Basel, Switzerland. This article is an open access article distributed under the terms and conditions of the Creative Commons Attribution (CC BY) license (<https://creativecommons.org/licenses/by/4.0/>).

## 1. Introduction

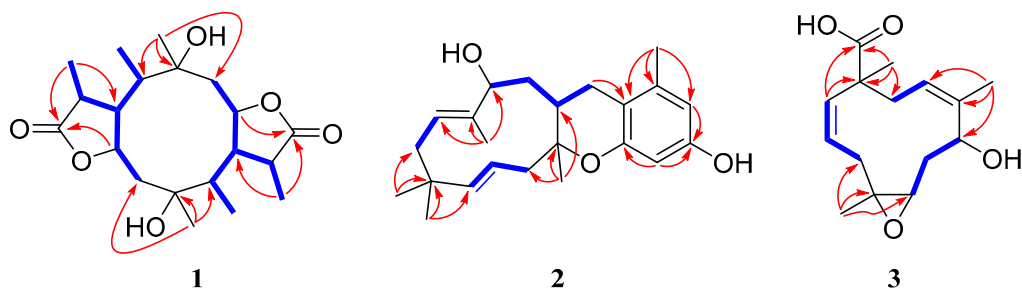
Mangrove endophytic fungi are the second largest ecological group of the marine fungi [1]. The particular environmental conditions of mangroves allow the activation of unique metabolic pathways in endophytic fungi, enabling the production of novel chemical backbones with diverse biological activities, making them a promising source of drug leads [2–5]. *Diaporthe* is a ubiquitous fungus commonly isolated from most plant hosts [6]. It is known to produce diverse compounds with antibacterial [7], antifungal [6], cytotoxic [8], antitubercular [9], antiparasitic [10] and anticancer [11] activities. With the aim of seeking new bioactive natural products from marine microorganisms, a mangrove endophytic fungus *Diaporthe* sp. QYM12, which was isolated from *Kandelia candel* collected from the South China Sea, was cultured in solid rice medium. As a result, six new metabolites including diaporpenoids A–C (**1–3**) and diaporpyrones A–C (**4–6**) together with one known analogue, 4-O-methylgermicidin L (**7**) [12], were isolated (Figure 1). Herein, the isolation, structure elucidation and anti-inflammatory activity of all isolated compounds are described.



**Figure 1.** The structures of 1–7.

## 2. Results

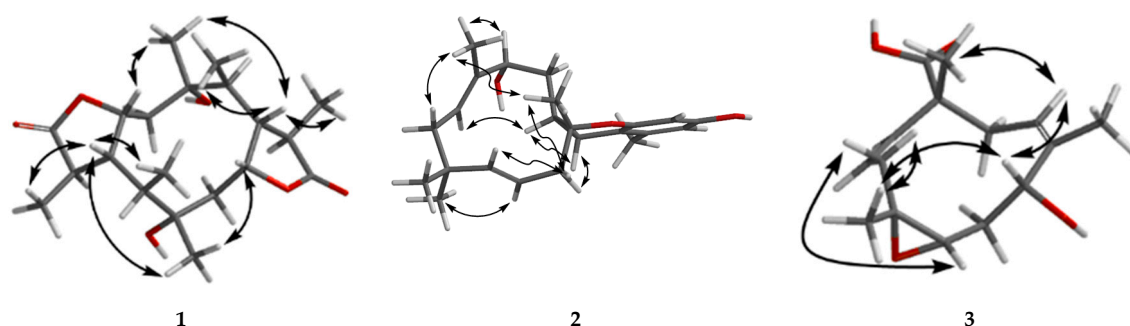
Compound **1** has a molecular formula of  $C_{20}H_{32}O_6$  based on the (+)-HRESIMS ( $m/z$ : 391.20900  $[M + Na]^+$ ), requiring five indices of hydrogen deficiency. The  $^1H$  NMR data (Table 1) showed six methyl signals at  $\delta_H$  1.20 (s,  $H_3$ -11), 1.33 (d,  $J = 7.6$  Hz,  $H_3$ -14), 0.97 (d,  $J = 7.3$  Hz,  $H_3$ -15), 1.22 (s,  $H_3$ -16), 1.31 (d,  $J = 7.3$  Hz,  $H_3$ -19) and 0.99 (d,  $J = 7.2$  Hz,  $H_3$ -20). Twenty carbon resonances in the  $^{13}C$  NMR data showed six methyls, two  $sp^3$  methylenes, eight  $sp^3$  methines and four quaternary carbons (two carbonyl carbons). These data suggested that **1** may be a tricyclic diterpenoid. The  $^1H$ - $^1H$  COSY spectrum revealed two spin systems:  $H_2$ -2/ $H$ -3/ $H$ -4(/ $H$ -5)/ $H$ -13/ $H_3$ -14 and  $H_2$ -7/ $H$ -8/ $H$ -9(/ $H$ -10)/ $H$ -18/ $H_3$ -19. The HMBC correlations (Figure 2) from  $H_3$ -11 to C-1, C-2 and C-10, and from  $H_3$ -16 to C-5, C-6 and C-7 implied the existence of a ten-membered ring core structure. Moreover, the correlations from  $H$ -3 to C-12, from  $H_3$ -14 to C-4 and C-12, from  $H_3$ -19 to C-9 and C-17, and from  $H$ -8 to C-17 were consistent with the existence of two five-membered lactones. The NOESY correlations (Figure 3) from  $H_3$ -11/  $H$ -3,  $H_3$ -11/  $H$ -9,  $H$ -9/ $H_3$ -20,  $H$ -9/ $H_3$ -19,  $H$ -4/  $H_3$ -16,  $H$ -4/  $H_3$ -15,  $H$ -4/  $H_3$ -14 and  $H_3$ -16/ $H$ -8 suggested that these protons were cofacial. Thus, the relative configuration of **1** has two possible enantiomers: **1a** (1*R*, 3*S*, 4*S*, 5*R*, 6*R*, 8*S*, 9*S*, 10*R*, 13*S*, 18*S*) and **1b** (1*S*, 3*R*, 4*R*, 5*S*, 6*S*, 8*R*, 9*R*, 10*S*, 13*R*, 18*R*). Comparing the experimental and calculated ECD spectra (Figure 4) between **1** and **1b** at the level of B3LYP/DGDZVP determined the absolute configuration of **1** as 1*S*, 3*R*, 4*R*, 5*S*, 6*S*, 8*R*, 9*R*, 10*S*, 13*R*, 18*R*.



**Figure 2.** Key HMBC (red arrows) and COSY (blue bold lines) correlations of 1–3.

**Table 1.**  $^1\text{H}$  and  $^{13}\text{C}$  NMR data for Compounds **1** and **2** in  $\text{CDCl}_3$ .

No.	1		2	
	$\delta_{\text{C}}$ , Type	$\delta_{\text{H}}$ (J in Hz)	$\delta_{\text{C}}$ , Type	$\delta_{\text{H}}$ (J in Hz)
1	80.9, C		137.8, C	
2	46.4, $\text{CH}_2$	2.16, m	108.9, CH	6.26, d (2.2)
3	81.5, CH	4.95, td (2.5, 7.3)	154.4, C	
4	54.1, CH	2.16, m	101.4, CH	6.18, d (2.3)
4a			154.5, C	
5	50.6, CH	1.96, dt (6.8, 13.2)	79.4, C	
6 $\alpha$	81.2, C		42.8, $\text{CH}_2$	2.51, d (14.5)
6 $\beta$				2.22, m
7	46.0, $\text{CH}_2$	2.21, m 2.05, m	121.3, CH	5.14, m
8	81.0, CH	4.86, td (2.5, 6.8)	141.4, CH	5.15, d (2.2)
9	49.6, CH	2.56, dt (7.2, 10.0)	38.5, C	
10	44.0, CH	2.05, m	40.6, $\text{CH}_2$	2.23, m 1.77, m 5.17, m
11	23.7, $\text{CH}_3$	1.20, s	123.5, CH	
12	181.1, C		138.6, C	
13	42.6, CH	2.72, qd (3.1, 7.6)	78.2, CH	3.99, d (9.6)
14 $\alpha$	18.3, $\text{CH}_3$	1.33, d (7.6)	39.7, $\text{CH}_2$	1.76, m
14 $\beta$				1.11, dd (9.3, 13.5)
14a			34.2, CH	1.69, m
15 $\alpha$	15.9, $\text{CH}_3$	0.97, d (7.3)	27.3, $\text{CH}_2$	2.88, dd (5.6, 16.4)
15 $\beta$				2.24, m
15a			112.7, C	
16	23.8, $\text{CH}_3$	1.22, s	19.3, $\text{CH}_3$	2.19, s
17	180.5, C		19.8, $\text{CH}_3$	1.06, s
18	38.3, CH	2.90, dq (7.3, 9.9)	24.1, $\text{CH}_3$	1.01, s
19	11.6, $\text{CH}_3$	1.31, d (7.3)	30.4, $\text{CH}_3$	1.06, s
20	15.8, $\text{CH}_3$	0.99, d (7.2)	10.6, $\text{CH}_3$	1.65, s

**Figure 3.** NOESY correlations of **1–3**.

Compound **2** was isolated as a colorless oil and had a molecular formula of  $\text{C}_{23}\text{H}_{32}\text{O}_3$  via HRESIMS. The NMR data of **2** were similar to those of pughiinin A [13]. It was confirmed that **2** had the same planar structure as pughiinin A by analyzing the COSY and HMBC correlations (Figure 2). The main difference was the 11*E*-configuration of the double bond between C-11 and C-12, which was confirmed by the NOESY correlation (Figure 3) from H $\alpha$ -10/H<sub>3</sub>-20. The chemical shift at C-20 ( $\delta_{\text{C}}$  10.6) in **2** further supported the 11*E*-configuration [14]. The relative configuration of **2** was elucidated by the NOESY correlations from H-13/H<sub>3</sub>-20, H<sub>3</sub>-20/H<sub>3</sub>-17, H<sub>3</sub>-17/H-6 $\beta$ , H-6 $\alpha$ /H-15 $\alpha$  and H-15 $\alpha$ /H-14a. Thus, the structure of **2** was defined as shown in Figure 1.

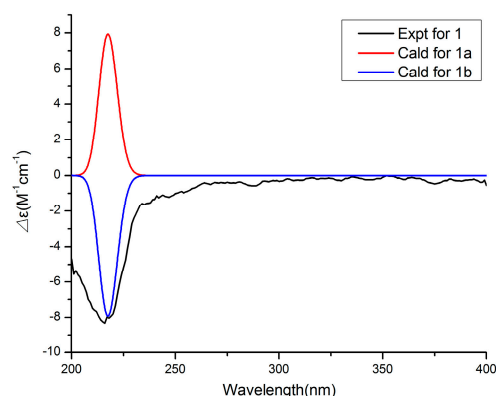


**Figure 4.** Comparison of the experimental and calculated ECD spectra of **1**.

The HRESIMS data of **3** suggested a molecular formula of  $C_{15}H_{22}O_4$ . The  $^{13}C$  NMR data (Table 2) showed 15 carbon resonances, including three methyls, three  $sp^3$  methylenes, five methines (two oxygen-bearing and three olefinic) and four quaternary carbons (one olefinic and one carbonyl). The COSY correlations (Figure 2) revealed the presence of three spin systems from H-1/H-2/H<sub>2</sub>-3, H-5/H<sub>2</sub>-6/H-7 and H-9/H<sub>2</sub>-10. The HMBC correlations from H<sub>3</sub>-12 to C-3, C-4 and C-5, H<sub>3</sub>-13 to C-7, C-8 and C-9, H<sub>3</sub>-14 to C-10, C-11 and C-15, and H-1 to C-11 and C-15 established the 11-membered ring core structure. The presence of a 4,5-oxirane ring was determined by the chemical shift values of C-4 ( $\delta_C$  64.6) and C-5 ( $\delta_C$  60.7). The NOESY correlations (Figure 3) from Ha-3/H-5, Hb-3/H<sub>3</sub>-12, H<sub>3</sub>-12/H-7, H-7/H-9 and H-9/H<sub>3</sub>-14 indicated the relative configuration as 4*R*\*, 5*R*\*, 7*R*\*, 11*R*\*. The limited quantity did not allow one to define the absolute configuration of **3** through the modified Mosher's method.

**Table 2.**  $^1H$  and  $^{13}C$  NMR data for **3** and **4** in MeOH- $d_4$ .

No.	<b>3</b>		No.	<b>4</b>	
	$\delta_C$ , Type	$\delta_H$ (J in Hz)		$\delta_C$ , Type	$\delta_H$ (J in Hz)
1	138.8, CH	5.50, d (15.8)	2	167.7, C	
2	124.6, CH	5.45, ddd (4.7, 10.6, 15.8)	3	97.8, C	
3 $\alpha$	44.1, CH <sub>2</sub>	2.60, dd (4.7, 11.9)	4	166.4, C	
3 $\beta$		1.57, dd (10.6, 11.9)	5	101.7, CH	6.06, s
4	64.6, C		6	160.0, C	
5	60.7, CH	2.45, dd (5.2, 9.7)	7	41.4, CH <sub>2</sub>	2.65, m
6 $\alpha$	34.4, CH <sub>2</sub>	2.19, ddd (5.1, 10.0, 13.3)	8	69.8, CH	4.47, d (6.5)
6 $\beta$		1.61, m	9	127.7, CH	5.58, dd (6.8, 15.6)
7	76.4, CH	4.10, dd (6.6, 10.1)	10	135.8, CH	6.25, d (15.6)
8	137.3, C		11	131.6, C	
9	126.5, CH	5.16, brd (11.4)	12	139.6, CH	5.23, d (10.0)
10 $\alpha$	36.4, CH <sub>2</sub>	2.71, dd (12.2, 13.3)	13	34.2, CH	2.40, m
10 $\beta$		2.08, brd (12.2)	14 $\alpha$	30.1, CH <sub>2</sub>	1.38, m
11	49.1, C		14 $\beta$		1.24, m
12	17.0, CH <sub>3</sub>	1.34, s	15	10.9, CH <sub>3</sub>	0.83, t (7.4)
13	10.8, CH <sub>3</sub>	1.64, s	16	19.6, CH <sub>3</sub>	0.94, d (6.6)
14	19.7, CH <sub>3</sub>	1.39, s	17	11.5, CH <sub>3</sub>	1.74, s
15	181.5, C		18	6.8, CH <sub>3</sub>	1.85, s

Compound **4** was assigned the molecular formula  $C_{17}H_{24}O_4$  by the HRESIMS ( $m/z$ : 291.16021 [ $M - H$ ] $^-$ ). The  $^1H$  NMR data (Table 2) exhibited the presence of four methyl signals at  $\delta_H$  0.83 (t,  $J$  = 7.4 Hz, 3H), 0.94 (d  $J$  = 6.6 Hz, 3H), 1.74 (s, 3H) and 1.85 (s, 3H), and four olefinic proton signals at  $\delta_H$  6.06 (s, 1H), 5.58 (dd,  $J$  = 6.8, 15.6 Hz, 1H), 6.25 (d,  $J$  = 15.6 Hz, 1H) and 5.23 (d,  $J$  = 10.0 Hz, 1H). The  $^{13}C$  NMR data revealed 17 carbon resonances including four methyls, two methylenes, six methines (four olefinic carbons)

and five other carbons (one carbonyl carbon and two olefinic carbons). Similar NMR data suggested that the structure of **4** was similar to that of proasperfuranone B [15]. The main difference was that the ketone carbonyl group in proasperfuranone B was reduced to a hydroxyl group in **4**. The deduction was confirmed by the HMBC correlations from H-8 to C-6, C-7 and C-9 (Figure 5). Thus, the planar structure of **4** was established. The calculated ECD spectrum fit the experimental spectrum perfectly well (Figure 6) at the BVP86/LANL2MB level in methanol; the absolute configuration of C-8 was determined as 8*R*.

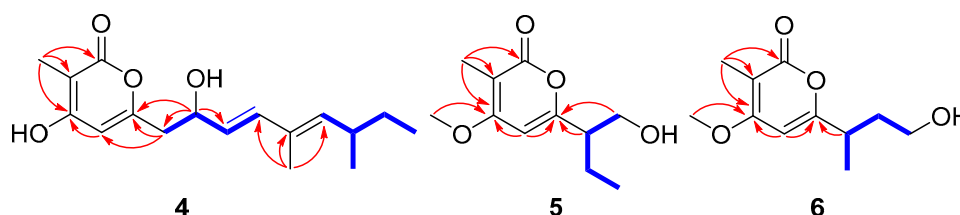


Figure 5. Key HMBC (red arrows) and COSY (blue bold lines) correlations of **4**–**6**.

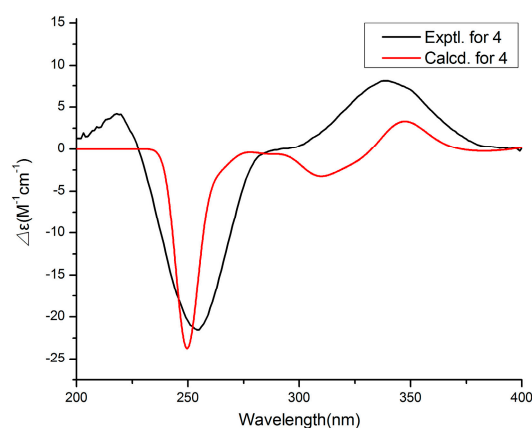


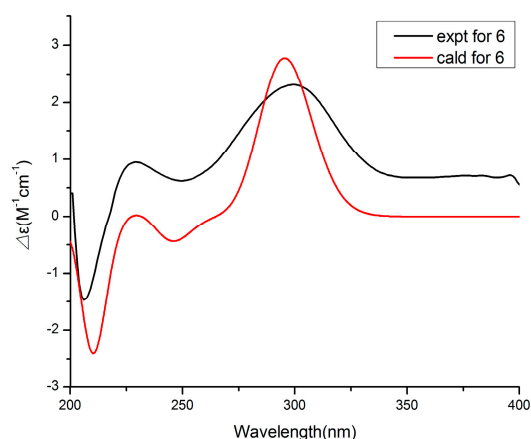
Figure 6. Experimental and calculated ECD spectra of **4**.

Compound **5**, isolated as a colorless oil, gave a molecular formula of  $C_{11}H_{16}O_4$  by HRESIMS data. The  $^1H$  NMR data (Table 3) exhibited the presence of three methyl signals at  $\delta_H$  0.92 (t,  $J = 7.4$  Hz, 3H), 1.91 (s, 3H) and 3.90 (s, 3H), and one olefinic proton at  $\delta_H$  6.10 (s, 1H). The  $^{13}C$  NMR data showed 11 carbon resonances assigned to two methyls ( $\delta_C$  8.5, 11.7), one methoxy ( $\delta_C$  56.2), two methylenes ( $\delta_C$  63.6, 22.1), two methines ( $\delta_C$  96.2, 49.4) and four nonprotonated carbons ( $\delta_C$  165.6, 101.3, 163.9 and 165.5). The HMBC correlations from H<sub>3</sub>-11 to C-2, C-3 and C-4, and H-5 to C-4 and C-6 revealed the presence of the  $\alpha$ -pyrone moiety. The correlations from H-7 and H-8 to C-6, as well as the  $^1H$ - $^1H$  COSY cross-peaks of H<sub>2</sub>-8/H-7/H<sub>2</sub>-9/H<sub>3</sub>-10 (Figure 5) indicated the side chain attached to C-6. Thus, the planar structure of **5** was established. By comparing the specific rotation value of **5** ( $[\alpha]_D^{25} -32$ ,  $c$  0.28, MeOH) with 4-deoxyphomapyrone C ( $[\alpha]_D^{25} -40$ ,  $c$  0.37, MeOH) [16] and germicidin C ( $[\alpha]_D^{25} +21$ ,  $c$  0.36, MeOH) [17], the absolute configuration of **5** was assigned as 7*R*.

**Table 3.**  $^1\text{H}$  and  $^{13}\text{C}$  NMR data for **5–7** in  $\text{CDCl}_3$ .

No.	5		6	
	$\delta_{\text{C}}$ , Type	$\delta_{\text{H}}$ (J in Hz)	$\delta_{\text{C}}$ , Type	$\delta_{\text{H}}$ (J in Hz)
2	165.6, C		166.2, C	
3	101.3, C		101.2, C	
4	163.9, C		166.2, C	
5	96.2, CH	6.10, s	93.8, CH	6.25, s
6	165.5, C		167.6, C	
7	49.4, CH	2.56, m	35.5, CH	2.82, dq (6.8, 13.7)
8	63.6, $\text{CH}_2$	3.88, m	37.4, $\text{CH}_2$	1.93, m
				1.75, dt (6.1, 13.6)
9	22.1, $\text{CH}_2$	1.65, m	60.3, $\text{CH}_2$	3.63, m
10	11.7, $\text{CH}_3$	0.92, t (7.4)	18.7, $\text{CH}_3$	1.25, d (6.9)
11	8.5, $\text{CH}_3$	1.91, s	8.5, $\text{CH}_3$	1.87, s
12	56.2, $\text{CH}_3$	3.90, s	56.4, $\text{CH}_3$	3.86, s

Compound **6** was obtained as a colorless oil and had a molecular formula of  $\text{C}_{11}\text{H}_{16}\text{O}_4$  by HRESIMS. The  $^1\text{H}$  and  $^{13}\text{C}$  NMR data (Table 3) of **6** were similar to those of **5**, revealing an  $\alpha$ -pyrone derivative. Moreover, the planar structure of **6** was established by the spin system of  $\text{H}_3\text{-10}/\text{H-7}/\text{H}_2\text{-8}/\text{H}_2\text{-9}$  from  $^1\text{H}\text{-}^1\text{H}$  COSY spectra together with the HMBC correlations (Figure 5) from H-7 and  $\text{H}_2\text{-8}$  to C-6. Meanwhile, the planar structure of **6** was identified as being the same as phomopyronol [18]. Finally, the calculated ECD spectrum and the experimental data (Figure 7) were well matched, indicating the 7R configuration of **6**.

**Figure 7.** Experimental and calculated ECD spectra of compound **6**.

Compound **7** was identified as 4-*O*-methylgermicidin L (**7**) [12] by a comparison of the spectroscopic data with the literature.

Nitric oxide (NO) is a key biological signaling molecule regulating the variety of physiological functions [19]. The excessive production of NO could induce tissue damage, and it is essential to find new effective NO inhibitors to treat inflammatory diseases and related disorders. Thus, the anti-inflammatory activity of isolated compounds was evaluated against nitric oxide (NO) production in lipopolysaccharide (LPS)-stimulated mouse macrophage RAW 264.7 cells. The results (Table 4 and Table S1) showed that **4** exhibited a potent inhibitory activity with an  $\text{IC}_{50}$  value of 12.5  $\mu\text{M}$ . Compounds **1–2** showed a moderate activity with  $\text{IC}_{50}$  values of 21.5 and 36.8  $\mu\text{M}$ , respectively, when compared to the positive control ( $\text{L-NMMA}$ ,  $\text{IC}_{50}$ : 15.0  $\mu\text{M}$ ). All the tested compounds were nontoxic at the tested concentration.



**Table 4.** The anti-inflammatory activities of compounds 1–8.

Compound	1	2	3	4	5	6	7	L-NMMA <sup>a</sup>
IC <sub>50</sub> (μM)	21.5	36.8	50.0	12.5	-	-	50.0	15.0

- not tested. <sup>a</sup> positive control.

### 3. Experimental Section

#### 3.1. General Experimental Procedures

Specific rotations were taken on a MCP 300 (Anton Paar) polarimeter at 28 °C. UV spectra were recorded in MeOH using a PERSEE TU-1900 spectrophotometer, and ECD data were measured on a Chirascan CD spectrometer (Applied Photophysics). IR spectra were obtained on a Nicolet Nexus 670 spectrophotometer, in KBr discs. All NMR experiments were performed on a Bruker Avance 500 spectrometer at room temperature. HRESIMS spectra were obtained on a Thermo Fisher Scientific Q-TOF mass spectrometer. Column chromatography (CC) was conducted using silica gel (200–300 mesh, Qingdao Marine Chemical Factory) and Sephadex LH-20 (Amersham Pharmacia). Semipreparative HPLC was carried out using a C18 column (ODS, 250 × 10 mm, 5 μm). Thin-layer chromatography (TLC) was performed on silica gel plates (Qingdao Huang Hai Chemical Group Co., G60, F-254).

#### 3.2. Fungal Material, Fermentation and Isolation

The strain QYM12 was isolated from the healthy leaves of *Kandelia candel*, which were collected in June 2017 from the South China Sea, Dongzhai Harbor Mangrove Nature Reserve Area, Hainan Province, China. Fungal identification was achieved using a molecular biological protocol by DNA amplification and ITS sequence [20]. The sequence was the most similar (99%) to the sequence of *Diaporthe* sp. (GU066666.1) via BLAST research. The sequence data of the strain has been deposited at GenBank with the accession number MW332459. The fungus was preserved at Sun Yat-Sen University, China. The strain was cultured on PDA medium for four days. Then, the seed culture was prepared by the mycelia of the fungus being inoculated into 500 mL of PDB medium for five days. Thereafter, the seed culture was transferred into solid rice medium (800 × 1000 Erlenmeyer flasks each containing 80 g of raw rice and 70 mL of 0.3% seawater) at 28 °C for 30 days.

Thereafter, the fermented material was extracted with MeOH three times, and organic phases were combined and evaporated under reduced pressure to yield an extract of 25.0 g. Then, the residue was fractionated by silica gel column chromatography with a gradient of petroleum ether/EtOAc from 10:0 to 0:10 to give eight fractions (Fr.1–Fr.8, per 10 mL). Fr.3 (380.0 mg) was subjected to Sephadex LH-20 CC (CH<sub>2</sub>Cl<sub>2</sub>/MeOH *v/v*, 1:1) to yield three fractions (3.1–3.3). Fr.3.1 (10.0 mg) was purified by silica gel CC (CH<sub>2</sub>Cl<sub>2</sub>/MeOH *v/v*, 75:1) to yield compound 1 (3.5 mg). Fr.4 (565.0 mg) was subjected to Sephadex LH-20 CC (CH<sub>2</sub>Cl<sub>2</sub>/MeOH *v/v*, 1:1) to yield two fractions (4.1 and 4.2). Fr.4.1 (36.5 mg) was purified by semipreparative reversed-phase HPLC (MeOH–H<sub>2</sub>O, 50:1) to yield compound 7 (3.1 mg). Fr.4.2 (46.2 mg) was subjected to silica gel CC (CH<sub>2</sub>Cl<sub>2</sub>/MeOH *v/v*, 95:5) to yield compounds 2 (2.0 mg) and 5 (5.6 mg). Fr.5 (522.0 mg) was purified by Sephadex LH-20 CC (CH<sub>2</sub>Cl<sub>2</sub>/MeOH *v/v*, 1:1) to afford three fractions (5.1–5.3). Fr.5.1 (7.6 mg) was subjected to silica gel CC (CH<sub>2</sub>Cl<sub>2</sub>/MeOH *v/v*, 25:1) to give compound 3 (2.0 mg). Fr.6 (650.0 mg) was subjected to Sephadex LH-20 CC (CH<sub>2</sub>Cl<sub>2</sub>/MeOH *v/v*, 1:1) to give four fractions (6.1–6.4). Fr.6.1 (38.0 mg) was purified by silica gel CC (CH<sub>2</sub>Cl<sub>2</sub>/MeOH *v/v*, 10:1) to yield compound 6 (6.8 mg). Fr.6.2 (15.0 mg) was subjected to silica gel CC (CH<sub>2</sub>Cl<sub>2</sub>/MeOH *v/v*, 17:3) to yield compound 4 (3.3 mg).

Diaporpenoid A (1): colorless oil;  $[\alpha]_D^{25}$  −32 (c 0.46, MeOH); UV (MeOH)  $\lambda_{\max}$  (log  $\epsilon$ ): 215 (2.52) nm; IR (KBr)  $\nu_{\max}$ : 3376, 2910, 2896, 1685, 1413, 1352, 1206, 1026 cm<sup>−1</sup>; <sup>1</sup>H and <sup>13</sup>C NMR (500 MHz, CDCl<sub>3</sub>) data, Table 1; HRESIMS *m/z* 391.20900 [M + Na]<sup>+</sup> (calcd for C<sub>20</sub>H<sub>32</sub>O<sub>6</sub>Na, 391.20911).

Diaporpenoid B (**2**): colorless oil;  $[\alpha]_D^{25} +28$  (c 0.06,  $\text{CDCl}_3$ ); UV (MeOH)  $\lambda_{\text{max}}$  (log  $\epsilon$ ): 209 (1.86), 281 (3.02) nm; IR (KBr)  $\nu_{\text{max}}$ : 3422, 3268, 2798, 1632, 1590, 1330, 1215, 1063  $\text{cm}^{-1}$ ;  $^1\text{H}$  and  $^{13}\text{C}$  NMR (500 MHz,  $\text{CDCl}_3$ ) data, see Table 1; HRESIMS  $m/z$  357.24244  $[\text{M} + \text{H}]^+$  (calcd for  $\text{C}_{20}\text{H}_{32}\text{O}_6$ , 357.24242).

Diaporpenoid C (**3**): colorless oil;  $[\alpha]_D^{25} +18$  (c 0.04, MeOH); UV (MeOH)  $\lambda_{\text{max}}$  (log  $\epsilon$ ): 220 (2.52) nm; IR (KBr)  $\nu_{\text{max}}$ : 3320, 1762, 1525, 1376, 1356, 1132, 1010  $\text{cm}^{-1}$ ;  $^1\text{H}$  and  $^{13}\text{C}$  NMR (500 MHz,  $\text{MeOH}-d_4$ ) data, see Table 2; HRESIMS  $m/z$  265.14401  $[\text{M} - \text{H}]^-$  (calcd for  $\text{C}_{15}\text{H}_{22}\text{O}_4$ , 265.14453).

Diaporpyrane A (**4**): colorless oil;  $[\alpha]_D^{25} +12$  (c 0.07, MeOH); UV (MeOH)  $\lambda_{\text{max}}$  (log  $\epsilon$ ): 212 (3.22), 240 (3.53) nm; IR (KBr)  $\nu_{\text{max}}$ : 3420, 2986, 2855, 1762, 1727, 1612, 1344, 1235, 1086  $\text{cm}^{-1}$ ;  $^1\text{H}$  and  $^{13}\text{C}$  NMR (500 MHz,  $\text{MeOH}-d_4$ ) data, see Table 2; HRESIMS  $m/z$  291.16021  $[\text{M} - \text{H}]^-$  (calcd for  $\text{C}_{17}\text{H}_{24}\text{O}_4$ , 291.16018).

Diaporpyrane B (**5**): colorless oil;  $[\alpha]_D^{25} -32$ , (c 0.28, MeOH); UV (MeOH)  $\lambda_{\text{max}}$  (log  $\epsilon$ ): 212 (3.45), 283 (3.62) nm; IR (KBr)  $\nu_{\text{max}}$ : 3176, 2965, 1647, 1580, 1421  $\text{cm}^{-1}$ ;  $^1\text{H}$  and  $^{13}\text{C}$  NMR (500 MHz,  $\text{CDCl}_3$ ) data, see Table 3; HRESIMS  $m/z$  213.11221  $[\text{M} + \text{H}]^+$  (calcd for  $\text{C}_{11}\text{H}_{17}\text{O}_4$ , 213.11214).

Diaporpyrane C (**6**): colorless oil;  $[\alpha]_D^{25} -65$  (c 0.85, MeOH); UV (MeOH)  $\lambda_{\text{max}}$  (log  $\epsilon$ ): 205 (3.32), 300 (3.67) nm; IR (KBr)  $\nu_{\text{max}}$ : 3445, 2962, 1735, 1675, 1363, 1256, 1218  $\text{cm}^{-1}$ ;  $^1\text{H}$  and  $^{13}\text{C}$  NMR (500 MHz,  $\text{CDCl}_3$ ) data, see Table 3; HRESIMS  $m/z$  213.1116  $[\text{M} + \text{H}]^+$  (calcd for  $\text{C}_{11}\text{H}_{17}\text{O}_4$ , 213.1117).

### 3.3. ECD Calculation Methods

The calculation was accomplished according to the method described previously [21]. The conformers of compounds **1**, **4** and **6** were first optimized by DFT methods at the B3LYP/6-31G (d) level in the Gaussian 05 program. Then, the theoretical calculation was performed using the time-dependent density functional theory (TD-DFT) at the level of B3LYP/DGDZVP, BVP86/LANL2MB and B3LYP/DGTZVP, respectively.

### 3.4. Anti-Inflammatory Assay

The method for the assay of the anti-inflammatory activity was conducted according to a previously published paper [20]. The detailed process is described in the Supplementary Materials.

## 4. Conclusions

In summary, the strain *Diaporthe* sp. QYM12, which was isolated from *Kandelia candel*, Dongzhai Harbor Mangrove Nature Reserve Area, was cultured in solid rice medium, leading to the identification of six new metabolite diaporpenoids A–C (**1–3**) and diaporpyranes A–C (**4–6**). Compound **1** was a macrocyclic diterpenoid featuring a rare 5/10/5-fused tricyclic ring system, and compounds **2,3** were macrocyclic sesquiterpenoids possessing a hendecane core. Macrocyclic sesquiterpenoids and diterpenoids are a functionally diverse group of natural products with versatile bioactivities [22]. For instance, junceollolide C showed an anti-HBV activity [23], flaccidenol A displayed a cytotoxic activity [24], antipacid B exhibited an anti-inflammatory activity [25], and euphorbesulins A revealed an antimalarial activity [26]. The anti-inflammatory assay suggested that compound **1** showed a moderate activity with an  $\text{IC}_{50}$  value of 21.5  $\mu\text{M}$ . Compound **4** exhibited a potent inhibitory activity with an  $\text{IC}_{50}$  value of 12.5  $\mu\text{M}$ . Proinflammatory enzymes, including nitric oxide synthase (iNOS) and cyclooxygenase-2 (COX-2), were reported to play key roles in inflammatory processes [27]. Thus, further research is required to clarify the underlying mechanisms of the active compounds. This study has suggested that these macrocyclic sesquiterpenoids and  $\alpha$ -pyrone derivatives have the potential to develop lead compounds for anti-inflammatory agents.



**Supplementary Materials:** The following are available online at <https://www.mdpi.com/1660-3397/19/2/56/s1>. Figure S1:  $^1\text{H}$  NMR spectrum of compound 1 (500 MHz,  $\text{CDCl}_3$ ). Figure S2:  $^{13}\text{C}$  NMR spectrum of compound 1 (125 MHz,  $\text{CDCl}_3$ ). Figure S3: HSQC spectrum of compound 1. Figure S4:  $^1\text{H}$ - $^1\text{H}$  COSY spectrum of compound 1. Figure S5: HMBC spectrum of compound 1. Figure S6: HRESIMS spectrum of compound 1. Figure S7: NOESY spectrum of compound 1. Figure S8:  $^1\text{H}$  NMR spectrum of compound 2 (500 MHz,  $\text{CDCl}_3$ ). Figure S9:  $^{13}\text{C}$  NMR spectrum of compound 2 (125 MHz,  $\text{CDCl}_3$ ). Figure S10: HSQC spectrum of compound 2. Figure S11:  $^1\text{H}$ - $^1\text{H}$  COSY spectrum of compound 2. Figure S12: HMBC spectrum of compound 2. Figure S13: NOESY spectrum of compound 2. Figure S14: HRESIMS spectrum of compound 2. Figure S15:  $^1\text{H}$  NMR spectrum of compound 3 (500 MHz,  $\text{MeOH}-d_4$ ). Figure S16:  $^{13}\text{C}$  NMR spectrum of compound 3 (125 MHz,  $\text{MeOH}-d_4$ ). Figure S17: HSQC spectrum of compound 3. Figure S18:  $^1\text{H}$ - $^1\text{H}$  COSY spectrum of compound 3. Figure S19: HMBC spectrum of compound 3. Figure S20: NOESY spectrum of compound 3. Figure S21: HRESIMS spectrum of compound 3. Figure S22:  $^1\text{H}$  NMR spectrum of compound 4 (500 MHz,  $\text{MeOH}-d_4$ ). Figure S23:  $^{13}\text{C}$  NMR spectrum of compound 4 (125 MHz,  $\text{MeOH}-d_4$ ). Figure S24: HSQC spectrum of compound 4. Figure S25:  $^1\text{H}$ - $^1\text{H}$  COSY spectrum of compound 4. Figure S26: HMBC spectrum of compound 4. Figure S27: HRESIMS spectrum of compound 4. Figure S28:  $^1\text{H}$  NMR spectrum of compound 5 (500 MHz,  $\text{CDCl}_3$ ). Figure S29:  $^{13}\text{C}$  NMR spectrum of compound 5 (125 MHz,  $\text{CDCl}_3$ ). Figure S30: HSQC spectrum of compound 5. Figure S31:  $^1\text{H}$ - $^1\text{H}$  COSY spectrum of compound 5. Figure S32: HMBC spectrum of compound 5. Figure S33: HRESIMS spectrum of compound 5. Figure S34:  $^1\text{H}$  NMR spectrum of compound 6 (500 MHz,  $\text{CDCl}_3$ ). Figure S35:  $^{13}\text{C}$  NMR spectrum of compound 6 (125 MHz,  $\text{CDCl}_3$ ). Figure S36: HSQC spectrum of compound 6. Figure S37:  $^1\text{H}$ - $^1\text{H}$  COSY spectrum of compound 6. Figure S38: HMBC spectrum of compound 6. Figure S39: HRESIMS spectrum of compound 6.

**Author Contributions:** Y.C. performed the experiments and wrote the paper; G.Z., W.Y. and Q.T. participated in the experiments; Y.Z., C.M., J.W. and L.C. analyzed the data and discussed the result; W.K. and Z.S. reviewed the manuscript; Z.S. designed and supervised the experiments. All authors have read and agreed to the published version of the manuscript.

**Funding:** This research was funded by the National Natural Science Foundation of China (U20A2001, 21877133), Key Project of Natural Science Foundation of Guangdong Province (2016A030311026) and Key Project in Science and Technology Agency of Henan Province (212102311029) through their generous support.

**Institutional Review Board Statement:** Not applicable.

**Data Availability Statement:** Data is contained within the article and Supplementary Material.

**Conflicts of Interest:** The authors declare no conflict of interest.

## References

- Cheng, Z.S.; Pan, J.H.; Tang, W.C.; Chen, Q.J.; Lin, Y.C. Biodiversity and biotechnological potential of mangrove-associated fungi. *J. For. Res.* **2009**, *20*, 63–72. [CrossRef]
- Sebastianes, F.L.S.; Cabedo, N.; Aouad, N.E. 3-Hydroxypropionic Acid as an Antibacterial Agent from Endophytic Fungi *Diaporthe phaseolorum*. *Curr. Microbiol.* **2012**, *65*, 622–632. [CrossRef] [PubMed]
- Zhu, F.; Lin, Y.C. Marinamide, a novel alkaloid and its methyl ester produced by the application of mixed fermentation technique to two mangrove endophytic fungi from the South China Sea. *Chin. Sci. Bull.* **2006**, *51*, 1426–1430. [CrossRef]
- Rosario, N.; Maria, S.; Anna, A. Secondary Metabolites of Mangrove-Associated Strains of *Talaromyces*. *Mar. Drugs* **2018**, *16*, 12.
- Deshmukh, S.K.; Gupta, M.K.; Prakash, V. Mangrove-Associated Fungi: A Novel Source of Potential Anticancer Compounds. *J. Fungi* **2018**, *4*, 101. [CrossRef]
- Carvalho, C.R.D.; Ferreira-D'Silva, A.; Wedge, D.E. Antifungal activities of cytochalasins produced by *Diaporthe miriciae*, an endophytic fungus associated with tropical medicinal plants. *Can. J. Microbiol.* **2018**, *64*, 835–843. [CrossRef]
- Sousa, J.P.B.; Aguilar-Pérez, M.M.; Arnold, A.E. Chemical constituents and their antibacterial activity from the tropical endophytic fungus *Diaporthe* sp. F2934. *J. Appl. Microbiol.* **2016**, *120*, 1501–1508. [CrossRef]
- Yang, X.; Wu, P.; Xue, J. Cytochalasins from endophytic fungus *Diaporthe* sp. SC-J0138. *Fitoterapia* **2020**, *145*, 104611. [CrossRef]
- Dettrakul, S.; Kittakoop, P.; Isaka, M. Antimycobacterial pimarane diterpenes from the Fungus *Diaporthe* sp. *Bioorg. Med. Chem. Lett.* **2003**, *13*, 1253–1255. [CrossRef]
- Chepkirui, C.; Stadler, M. The genus *Diaporthe*: A rich source of diverse and bioactive metabolites. *Mycol. Prog.* **2017**, *16*, 477–494. [CrossRef]

11. Kumaran, R.S.; Hur, B.K. Screening of species of the endophytic fungus *Phomopsis* for the production of the anticancer drug taxol. *Biotechnol. Appl. Bioc.* **2011**, *54*, 21–30. [[CrossRef](#)] [[PubMed](#)]
12. Du, Y.; Sun, J.; Gong, Q. New  $\alpha$ -Pyridones with Quorum Sensing Inhibitory Activity from Diversity-Enhanced Extracts of a Marine Algae-Derived *Streptomyces* sp. *J. Agric. Food Chem.* **2018**, *66*, 1807–1812. [[CrossRef](#)] [[PubMed](#)]
13. Pittayakhajonwut, P.; Theerasilp, M.; Kongsaree, P.; Pughinin, A. A Sesquiterpene from the Fungus *Kionochaeta pughii* BCC 3878. *Planta Med.* **2002**, *68*, 1017–1019. [[CrossRef](#)] [[PubMed](#)]
14. Cai, P.; Smith, D.; Cunningham, B. Epolones: Novel Sesquiterpene-Tropolones from Fungus OS-F69284 That Induce Erythropoietin in Human Cells. *J. Nat. Prod.* **1998**, *61*, 791–795. [[CrossRef](#)] [[PubMed](#)]
15. Chiang, Y.M.; Oakley, C.E.; Ahuia, M. An efficient system for heterologous expression of secondary metabolite genes in *Aspergillus nidulans*. *J. Am. Chem. Soc.* **2013**, *135*, 7720–7731. [[CrossRef](#)] [[PubMed](#)]
16. Zhang, H.; Saurav, K.; Yu, Z.  $\alpha$ -Pyrones with Diverse Hydroxy Substitutions from Three Marine-Derived *Nocardiopsis* Strains. *J. Nat. Prod.* **2016**, *79*, 1610–1618. [[CrossRef](#)] [[PubMed](#)]
17. Aoki, Y.; Matsumoto, D.; Kawaide, H. Physiological role of germicidins in spore germination and hyphal elongation in *Streptomyces coelicolor* A3(2). *J. Antibiot.* **2011**, *64*, 607–611. [[CrossRef](#)]
18. Weber, D.; Gorzalczy, S.; Martino, V. Metabolites from Endophytes of the Medicinal Plant *Erythrina crista-galli*. *Z. Naturforsch. C. Biosci.* **2005**, *60*, 5–6. [[CrossRef](#)]
19. Iadecola, C.; Pelligrino, D.A.; Moskowitz, M.A. Nitric oxide synthase inhibition and cerebrovascular regulation. *J. Cereb. Blood Flow Metab.* **1994**, *14*, 175–192. [[CrossRef](#)]
20. Chen, Y.; Liu, Z.M.; Liu, H.J. Dichloroisocoumarins with Potential Anti-Inflammatory Activity from the Mangrove Endophytic Fungus *Ascomycota* sp. CYSK-4. *Mar. Drugs* **2018**, *16*, 54. [[CrossRef](#)]
21. Chen, Y.; Liu, Z.M.; She, Z.G. Ascomylactams A-C, Cytotoxic 12- or 13-Membered-Ring Macrocyclic Alkaloids Isolated from the Mangrove Endophytic Fungus *Didymella* sp. CYSK-4, and Structure Revisions of Phomapyrrolidones A and C. *J. Nat. Prod.* **2019**, *82*, 1752–1758. [[CrossRef](#)] [[PubMed](#)]
22. Thomas, B.; Robert, K.; Bernhard, L. Production of Macrocyclic Sesqui- and Diterpenes in Heterologous Microbial Hosts: A Systems Approach to Harness Nature's Molecular Diversity. *Chemcatchem* **2014**, *6*, 1142–1165.
23. Wu, J.R.; Li, X.D.; Lin, W.H. Briarane-type diterpenoids from a gorgonian coral *Ellisella* sp. with anti-HBV activities. *Bioorg. Chem.* **2020**, *105*, 104423. [[CrossRef](#)] [[PubMed](#)]
24. Tseng, W.-R.; Ahmed, A.F.; Huang, C.-Y.; Tsai, Y.-Y.; Tai, C.-J.; Orfali, R.S.; Hwang, T.-L.; Wang, Y.-H.; Dai, C.-F.; Sheu, J.-H. Bioactive Capnosanes and Cembranes from the Soft Coral *Klyxum flaccidum*. *Mar. Drugs* **2019**, *17*, 461. [[CrossRef](#)] [[PubMed](#)]
25. Chang, Y.C.; Chiang, C.C.; Chang, Y.S.; Chen, J.J. Novel Caryophyllane-Related Sesquiterpenoids with Anti-Inflammatory Activity from *Rumphella antipathes* (Linnaeus, 1758). *Mar. Drugs* **2020**, *18*, 554. [[CrossRef](#)]
26. Zhou, B.; Wu, Y.; Yue, J.M. Euphorbesulins A–P, Structurally Diverse Diterpenoids from *Euphorbia esula*. *J. Nat. Prod.* **2016**, *79*, 1952–1961. [[CrossRef](#)]
27. Lee, S.J.; Lee, I.S.; Mar, W. Inhibition of inducible nitric oxide synthase and cyclooxygenase-2 activity by 1,2,3,4,6-penta-O-galloyl-beta-D-glucose in murine macrophage cells. *Arch. Pharm. Res.* **2003**, *26*, 832–839. [[CrossRef](#)]